Judging for Barrier Lakes Based on Color Constancy Color Index Similarity Measure

Chunxue Wu[1], Bobo Ju[1], Yan Wu[2], Xiao Lin[3], Naixue Xiong[4]

[1] School of Optical-Electrical and Computer Engineering, University of Shanghai for Science and Technology, China
[2] O'Neill School of Public and Environmental Affairs, Indiana University Bloomington, USA
[3] Department of Computer Science, Shanghai Normal University, China
[4] College of Intelligence and Computing, Tianjin University, China
wcx@usst.edu.cn, xh11407130@outlook.com, yanwu8910@gmail.com, lin6008@126.com, naixuexiong@gmail.com

Abstract

The barrier lake is a very common secondary disaster. The way to judge the barrier lake in the past is to led expert to assess whether a barrier lake has occurred. In traditional computer vision research focusing on figure features, color has not received sufficient attention, and it is generally believed that color is not an essential feature of an object. However, for geometric features, the color has a certain stability, which is not sensitive to size and direction, and exhibits considerable robustness. At the same time, in many cases, color is the easiest and most effective feature to describe an image, and is one of the main methods used to measure content similarity. This paper analyzes the map formed by aerial photography of drones, and uses the color constancy color similarity measure color constant color index and binary image similarity measure to judge whether the river is blocked and the degree of blockage, instead of the previous artificial judgment on the barrier lake. The results show that the color constant color index water body extraction method is less affected by the mountain shadow and thin cloud, which can completely eliminate the "Noise water body" phenomenon caused by the pixel-based color constant color index water body extraction method.

Keywords: Color constancy color index, Gaussian Markov random field, Supervised color constancy, Minkowsky distance

1 Introduction

As we all known, the existence of the barrier lake is a very dangerous disaster. Because the water level in the barrier lake exceeds the warning value will lead the obstruction breaks. At this time, a large amount of water in the barrier lake will cause a devastating blow to the downstream city. Therefore, it is very important to detect (ie, warning and monitoring) the stagnation in the river in advance. In the past, the means of discovering the barrier lake often is that geologists to evaluate the river state after the earthquake, but this process is too slow and the results of the assessment are influenced by the level of expert knowledge. We want to reduce the amount of manual intervention in the interpretation of the barrier lake, using the more popular computer vision methods to identify and evaluate the barrier lake. Before introducing our research, a brief understanding of the following concepts is necessary to understand the entire paper.

The extraction of the underlying features of images is one of the most important functions in the content-based image similarity measurement system. Accurate extraction of image features plays an important role in the effect and speed of similarity measures. There are two broad categories of objects in an image: one that describes and identifies a single object or part of an object, such as color, texture, and shape. Among them, the color and texture features emphasize the color, grayscale change, shape of the surface of the object, the structural features emphasize the shape and size of the object, and the other is used to describe the composition of the object or the three-dimensional information of the object, such as left and right, far and near, perspective Wait. At present, it is generally believed that the underlying features of the image used by the Content Based Image Retrieval [1] (Referred to as CBIR) system mainly include two-dimensional visual information features such as texture and color.

1.1 Extraction Based on Color Features

Color is an inherent visual property of the surface of an object, so each image has its own unique color characteristics. Here, the color has rotation invariance and dimensional invariance, and the dependence on the size, direction and viewing angle of the image itself is small, so the color is the most widely used visual feature in the CBIR system [1]. Image similarity metrics using color features have become one of the most important methods based on content similarity measurement techniques. There are three key

*Corresponding Author: Chunxue Wu; E-mail: wcx@usst.edu.cn
DOI: 10.3966/160792642020032102025

techniques for measuring images using color feature similarity: selecting appropriate color models, effective feature extraction methods, and accurate feature matching algorithms [2].

1.2 Color-based Similarity Measurement Algorithm

The basic idea of the color-based similarity measurement algorithm is to perform color space histogram matching. The color space and matching method used vary with different algorithms [3]. In 1990, Swain and Ballard proposed the basic ideas and algorithms of the Color Similarity Index [4]. Object color histograms are used to describe objects, and object recognition (similarity measure) and localization in the image are accomplished by defining the intersection of the histogram and the Backprojection Algorithm [5-6]. After the histogram intersection algorithm is given to the specified image histogram, the color similarity measure becomes the image with the largest matching degree in the model library. Swain further proves that when the number of pixels of the two histograms is the same, the result of the histogram intersection operation reflects the city-block distance of the two histograms, which more fully explains the meaning of the algorithm [7].

The stability of the similarity measure relative to the illumination is an important feature of the color similarity measurement algorithm. The Swain algorithm is extremely sensitive to illumination conditions, and only the variation of the illumination amplitude will greatly affect the accuracy of the recognition algorithm. In his paper, he proposes to use Novak's Supervised Color Constancy algorithm, a swatch that prevents known reflectance in the environment as a reference for illumination changes. However, in many cases, this condition is difficult to meet [8-9]. Funt and Finalyson proposed a color constancy color similarity measure (Referred to as CCCI) algorithm for this case. Starting from Land's visual cortex theory, they advocated taking the logarithm of the input color image and then making a difference to weaken the influence of the illumination change, and then establishing a histogram on the color edge points obtained after the difference, as a match. standard. The experimental results show that their similarity measure algorithm is more robust than the Swain algorithm with illumination changes, but the similarity measure accuracy is not as good as Swain's similarity measure algorithm under the premise of illumination invariance [10].

The remainder of this paper is organized as follows: Section 2 points out the related work and the shortcomings that the predecessors have done in river feature extraction, and the work we still have to do, and some predecessors have done work on image color feature extraction which can be used by this research. At the end paragraph of this chapter, it presents the contribution of our research. Section 3 presents the proposed method which be used in our research, and introduces some classic image similarity measure. Section 4 gives datasets used in this study are presented, the specific experimental process using our research methods are recorded, and then the experimental and other existing methods are compared in the experimental analysis section. In Section 5, the overall process of this study was briefly summarized.

2 Related Work

In the field of remote sensing, methods for extracting river features using computer vision combined with other methods have been studied by related experts in the past. The feature extraction method of DEM[1] in ArcGIS[2] environment is based on the slope runoff simulation method provided by Marks and O'Callaghan [11], and the DEM water feature is extracted in ArcGIS environment. The application principle of this method is to first calculate the catchment area through the grid unit, and then determine the threshold of the catchment area for the river network. This method is equivalent to the path judgment of surface runoff. This is through the use of the confluence concept in hydrology, and the flow path will be continuously generated in this process, so this method in the water extraction process is a superior choice. Shen Li et al. proposes high-resolution remote sensing imagery river extraction combined with spatial pixel template and Adaboost algorithm [12]. This method eliminates a spatial pixel template to obtain spatial neighborhood relationship, and combines Adaboost integrated learning algorithm to achieve extract of accurate river resolution on remote sensing image. Xu and Hou also proposes a region-based remote sensing image river extraction method [13]. The method first generates a grayscale image based on the remote sensing image, selects the initial region of the river, sets the growth range and growth threshold, and obtains the river boundary through regional production, and proposes the river interior. "Island" and refine the border, and finally generate a vector file. This is a method of automatically extracting river information using images. These river feature extraction methods have performed very well in the ground information drawing. But these methods only can map the general position of the river in the remote sensing image. And it is not possible to identify details in rivers. For example, these methods cannot effectively extract the characteristics of the barrier lake

[1] Full name is Digital Elevation Model. Digital simulation of ground terrain (ie, digital representation of topographical surface morphology) through limited terrain elevation data

[2] This is a professional mapping software. Maps drawn with ArcGIS can not only display information, but also use it to support query, analysis, planning, and management.

mentioned in this paper. Therefore, researching a new method for extracting river features that can identify river anomalies is one of the focuses of this paper.

2.1 Color Space Model

The choice of the color space model directly affects the similarity measurement effect. Currently, the commonly used color space models include RGB color space, HSV color space and CIE color space.

According to the principle of three-color hypothesis, any color can be mixed by three different basic colors of red, green and blue according to different proportions. This color space composed of RGB three primary colors is called an RGB model [14].

The HSV color space directly corresponds to the three elements of human eye color vision, namely hue H (Hue), saturation S (Saturation) and brightness V (Value), and the channels are independent. Therefore, from the perspective of human psychology, the HSV color space directly reflects the way people observe color than the RGB space, and is more acceptable [15].

2.2 CIE Color System

Assuming that the difference between the two colors observed by a person in a color space corresponds to the Euclidean distance between two points in the color space, the space is said to be a uniform color space. Typical examples are the Luv model and the Lab model of the MTM model CIE [16-17].

2.3 Color Feature Expression

Color histograms have good performance, and can be based on different color spaces and coordinate systems, where HSV space is the most common color space for histograms. It describes the proportion of different colors in the entire image, and does not care about the spatial position of each color, reflecting the statistical distribution and basic color of the image color. Therefore, the color histogram is particularly suitable for describing images that are difficult to automatically segment and images that do not need to consider the spatial position of the object [18].

The statistical histogram of image features is actually a one-dimensional discrete function, namely: $H(k)=\frac{n_k}{N}\quad k=0,1,\ldots,L-1$ Where k represents the feature value of the image, L is the number of feature values, n_k is the number of pixels in the image with a feature value of k, and N is the total number of image pixels.

A color correlation graph is another way of expressing the spatial distribution of an image color using the color relationship between pixels in an image. The color correlation diagram not only depicts the proportion of pixels of a certain color in the entire image, but also reflects the spatial correlation of different colors. For the selected image I, assuming that I_{ci} represents a set of all pixels in the image with color $c(i)$, the color correlation graph can be expressed as $\gamma_{ci,cj}^{(k)}(I)\triangleq \Pr\left[p2\in I_{cj},|p1-p2|=k/p1\in I_{ci}\right]$ where $i,j\in\{1,2,\ldots,m\}$, m represents the image color progression, $k\in\{1,2,\ldots,d\}$, d represents the maximum distance between pixels set when calculating the relevant image of the image, and $|p1-p2|$ represents the distance between pixels p1 and p2. At this time, the color histogram can be regarded as a table indexed by color pairs $\langle i,j\rangle$, where the kth component of $\langle i,j\rangle$ indicates that the colors in the image are $c(i)$ and $c(j)$ and the distance The probability of occurrence of a pair of pixels of k. If you consider the correlation between any color, the color correlation graph will become very complicated and huge (the spatial complexity is $O(m^2d)$); if you consider the spatial relationship of pixels with the same color in the image space, then there is the color of I. The autocorrelation graph, expressed as $\alpha_c^k(I)\triangleq\ \gamma_{c,c}^k(I)$, has a spatial complexity of only $O(md)$.. Experiments show that the color correlation graph considers the color distribution and spatial information, and has higher similarity measurement efficiency than the color histogram [19].

Kankanhalli and Mehtre proposed a cluster-based color matching method, the main color method [20]. Depending on the visual characteristics of the person, the human eye is interested in the main color of the image. Then the main color refers to the color in the image which has a relatively high frequency and plays an important role in the expression of image semantic information.

In image processing, the main color extraction process is: first color space conversion. The image is transferred from the RGB space to the HSV space; then the HSV is quantized, and the color of the entire image after quantization can be represented by 162 ($18\times3\times3$) colors; finally, the normalized histogram is calculated. That is, the percentage of each color in the image is obtained, and the descriptor F is composed of the color and its corresponding percentage, $F=\{(c_i,p_i),i=1,2,3,\ldots,N,p_i\in[0,1]\}$. Where N is the total number of colors in the image, ci is the color, and pi is the percentage of it. The various colors (c_i) are arranged in descending order of their corresponding percentages (p_i), and the main color is obtained by the sequence, and one of the two conditions of $p_i\geq5\%$ or $\sum p_i\leq60\%$ is satisfied, and the color is taken as the main color. In addition, the MPEG-7 standard specifies.

The similarity between the two primary colors is

calculated as follows:

The two primary colors describe the distance between $F_1 = \{(c_{li}, p_{li}), i = 1,2,3,\ldots,N_1\}$ and $F_2 = \{(c_{2i}, p_{2i}), j = 1,2,3,\ldots,N_2\}$. $D^2(F_1,F_2) = \sum_{i=1}^{N_1} p_{1i}^2 + \sum_{j=1}^{N_2} p_{2j}^2 - \sum_{i=1}^{N_1}\sum_{j=1}^{N_2} 2a_{1i,2j}p_{1i}p_{2j}$ Where $a_{k,j}$ is the similarity of the two colors c_k, c_j, $a_{kj} = \begin{cases} 1 - d_{kj}/d_{\max}, d_{kj} \le T_d \\ 0, d_{kj} > T_d \end{cases}$. d_{kj} is the Euclidean distance of the two colors c_k, c_j. For the two colors of HSV space (h_i, s_i, v_i) and (h_j, s_j, v_j): $d_{kj} = \sqrt{(v_i - v_j)^2 + (s_i\cosh_i - s_j\cosh_j)^2 + (s_i\sinh_i - s_j\sinh_j)^2}$, $d_{\max}$ is the maximum distance between the two colors. By calculating two opposite colors, such as $(0^o, 1, 0)$ and $(180^o, 1, 1)$, you can get $d_{\max} = \sqrt{5}$.

The main color extraction algorithm not only reduces the number of color features, but also removes the color interference caused by unimportant objects, is not sensitive to noise and brightness, and does not depend on the prior knowledge of image color distribution, and can be more accurate [21]. The image color is expressed to achieve a balance of precision and dimensionality. The primary color information is finally represented by a variable histogram. It is simple to implement, especially suitable for image similarity metrics with obvious main color features [22].

This experiment is mainly for the analysis of remote sensing images. The rivers in remote sensing images are segmented by CCCI, and then the color similarity metrics are used to evaluate the similarity of rivers in the same region before and after the earthquake. If the binary image difference is too large, it is considered that the river in the area is blocked. This experiment also horizontally compares texture-based feature extraction + texture-based image similarity measurement method, and uses deep learning U-net neural network for image segmentation feature extraction + texture/color feature based image similarity measurement method. It shows that the latter two methods are not as good as the former. On the one hand, color differences are the best way to distinguish between rivers and complex backgrounds, and because complex textures in remote sensing images interfere with segmented rivers. On the other hand, because U-net is suitable for a large number of data samples, and the experimental data set is relatively small, even the method using the data set enhancement can't get a good effect [23-24]. So in this case, using CCCI is the best option.

3 Methods and Models

3.1 Using CCCI to Extract River Characteristics

First, you must create a histogram database. The combined proportion of each image is calculated as follows:

(1) Logarithmic steps:

$$i_k(x,y) \Leftarrow \ln(\rho_k(x,y)) \quad k = 1\ldots3 \tag{1}$$

(2) Differentiation convolution step (①, ② or ③):

①Laplacian

$$d_k(x,y) \Leftarrow \nabla^2 i_k(x,y) \quad k = 1\ldots3 \tag{2}$$

②Gaussian Laplacian

$$d_k(x,y) \Leftarrow \nabla^2 G * i_k(x,y) \quad k = 1\ldots3 \tag{3}$$

③four-way derivative

$$d_{m,k}(x,y) \Leftarrow \nabla_m i_k(x,y) \quad k = 1\ldots3, m = 1\ldots4 \tag{4}$$

Where m is the index direction.

(3) Histogram step (⑴ or ⑵)

①Gaussian Laplacian or Laplacian

$$H(i,j,k) \Leftarrow \sum_{x,y} z = \begin{cases} & d_1(x,y) = i \\ 1 \quad if & d_2(x,y) = j \\ & d_3(x,y) = k \\ 0 & otherwise \end{cases} \tag{5}$$

②4 directional derivatives

$$H(i,j,k) \Leftarrow \sum_{m=1}^{4}\sum_{x,y} z = \begin{cases} & d_{m,1}(x,y) = i \\ 1 \quad if & d_{m,3}(x,y) = j \\ & d_{m,3}(x,y) = k \\ 0 & otherwise \end{cases} \tag{6}$$

Once a database of ratio (or derived) histograms has been compiled for a set of known objects, it can be used to identify instances of one of these objects in the new image. Calculates the ratio histogram of the new image and then intersects each model histogram in the database [25-26]. The histogram intersection is performed according to (1), which is exactly the same as Swain.

Steps (1) and (2) represent the only additional calculations required to achieve illumination independence. The logarithm in step (1) can be done by table lookup in hardware, and the derivative operator of step (2) can be implemented as convolution. For this application, the derivative operator only needs relatively little support because the purpose is to compare the colors in a small area to avoid violating the assumption of constant illumination.

3.2 Similarity Measure Based on Color Features

Common similarity measures based on color features mainly include absolute distance, Euclidean distance, histogram intersection method, χ^2 distance, reference color table, center distance, and so on.

First, a,b is the feature vector corresponding to the two images, and a_i,b_i represents the feature component.

The Minkowsky distance is defined based on the L_p norm [27]:

$$L(A,B)=\left[\sum_{i=1}^{n}|a_i-b_i|^p\right]^{\frac{1}{p}} \tag{7}$$

(1) If p=1, it is called city-block, which is the absolute distance:

$$L_1(A,B)=\left[\sum_{i=1}^{n}|a_i-b_i|\right] \tag{8}$$

(2) If p=2, it is called Euclidean Distance:

$$L_2(A,B)=\left[\sum_{i=1}^{n}(a_i-b_i)^2\right]^{\frac{1}{2}} \tag{9}$$

If the components of the image feature are orthogonally independent and the importance of each dimension is the same, the distance between the two feature vectors can be measured by the Euclidean distance. In practical applications, in order to reduce the amount of calculation, the color information is often roughly expressed by means of the mean of the histogram. If the image is represented by three components of RGB, the feature vector of the image consists of the mean of the three components.

$$f=\left[\psi_R\psi_G\psi_B\right]^T \tag{10}$$

At this time, the similarity of image a,b is:

$$S(A,B)=\sqrt{(f_a-f_b)^2}=\sqrt{\sum_{R,G,B}(\psi_a-\psi_b)^2} \tag{11}$$

(3) If $p\to\infty$, called Chebyshev distance:

$$L_\infty(A,B)=\max_{i=1}^{n}|a_i-b_i| \tag{12}$$

The histogram intersection method was first proposed by Swain et al [28]. The histogram intersection method is simple and fast, and can better suppress the influence of the background. The mathematical description is:

$$d(A,B)=1-\sum_{i=1}^{n}\min(a_i,b_i) \tag{13}$$

The above formula can be further normalized:

$$d(A,B)=1-\frac{\sum_{i=1}^{n}\min(a_i,b_i)}{\min\left(\sum_{i=1}^{n}a_i\sum_{i=1}^{n}b_i\right)} \tag{14}$$

In practical application: Let $H_A(k)$ and $H_B(k)$ be the statistical histograms of the feature of the query image a and the database image b, respectively, and the similarity distance between the two images:

$$d_{Lk}(A,B)=1-\frac{\sum_{k=0}^{L-1}\min\{H_A(k),H_B(k)\}}{\sum_{k=0}^{L-1}H_A(k)} \tag{15}$$

Assuming that the HSV histogram represents each image, the similarity distances of the two images a and b are:

$$d_L(A,B)=1-\frac{\sum_H\sum_S\sum_V\min\{H_A(H,S,V),H_B(H,S,V)\}}{\min\left\{\sum_H\sum_S\sum_V\{H_A(H,S,V)\},\sum_H\sum_S\sum_V\{H_B(H,S,V)\}\right\}} \tag{16}$$

The above formula can be further normalized:

$$d_L(A,B)=1-\frac{\sum_H\sum_S\sum_V\min\{H_A(H,S,V),H_B(H,S,V)\}}{\sum_H\sum_S\sum_V H_A(H,S,V)} \tag{17}$$

For image histograms based on color histograms, quadratic distances have proven to be more efficient than Euclidean distance and histogram intersections because they take into account the existence of different colors Similarity [29]. There are two color histograms H_A and H_B, and the quadratic distance between them can be expressed as:

$$D(H_A,H_B)=(H_A-H_B)^T M(H_A-H_B) \tag{18}$$

Where $M=\begin{bmatrix}1 & s_{12} & \cdots & s_{1N}\\ s_{21} & 1 & \cdots & s_{2N}\\ \cdots & \cdots & s_{ij} & \cdots\\ s_{N1} & s_{N2} & \cdots & 1\end{bmatrix}$, s_{ij} represent the similarities between the two colors of the subscripts i and j in the histogram. This method can be obtained through the study of color psychology by introducing the color similarity matrix M so that it can take into account the similarity factors between similar but different colors.

The χ^2 statistical calculation similarity distance can be defined as:

$$d_{\chi^2}(A,B)=\sum_{i=0}^{N-1}\frac{(A_i-B_i)^2}{m_i} \quad (19)$$

Where A,B represents two images, $m_i=\frac{A_i+B_i}{2}$

For color images, the $i(i\le 3)$ step center distances of the histograms of the three components R, G, and B of the images A and B are represented by $M_{i,AR},M_{i,AG},M_{i,AB}$ and $M_{i,BR},M_{i,BG},M_{i,BB}$, and the matching values between them are:

$$P(A,B)=\sqrt{W_R\sum_{i=1}^{3}\left(M_{i,AR}-M_{i,BR}\right)^2+W_G\sum_{i=1}^{3}\left(M_{i,AG}-M_{i,BG}\right)^2+W_B\sum_{i=1}^{3}\left(M_{i,AB}-M_{i,BB}\right)^2} \quad (20)$$

If the color image is represented by 3 components H, S, V, it can also be calculated in a similar way.

The color of the image is represented by a set of reference colors that should cover the various colors that are visually perceived. The number of reference colors is smaller than the original image, and the histogram can be simplified, so the matching feature vector is: $f=[r_1,r_2,\ldots,r_n]$. r_i is the frequency at which the $i-th$ color appears, and n is the size of the reference color table. The matching value between the weighted query image A and the database image B is:

$$P(A,B)=W\sqrt{(f_A-f_B)^2}=\sqrt{\sum_{i=1}^{n}W_i\left(r_{i,A}-r_{i,B}\right)^2} \quad (21)$$

$$W_i=\begin{cases}r_{i,A} & \text{当} r_{i,A}>0 \text{且} r_{i,B}>0\\ 1 & \text{当} r_{i,A}=0 \text{且} r_{i,B}=0\end{cases} \quad (22)$$

3.3 Texture-based Similarity Measure

Common texture feature-based similarity metric calculation methods mainly include Euclidean distance and Mahalanobis distance. The Euclidean distance measurement method with the Euclidean distance and the color feature similarity measure is the same. See the Minkowsky distance p for 2.

If the components of the feature vector have correlation or have different weights, the Mahalanobis distance can be used to calculate the similarity between the features [30]. The mathematical expression of the Mahalanobis distance is:

$$D_{mahal}=(A-B)^T C^{-1}(A-B) \quad (23)$$

Where C is the covariance matrix of the feature vector.

The flow chart of this experiment is shown in Figure 1 above. The remote sensing image is used for pre-processing, and then CCCI/GMRF (Gaussian Markov random field) /U-net is used to extract the characteristics of the river before and after the blockage, and then the similarity of the image before and after the blockage is judged by using the method of judging image similarity.When the similarity is small, the river is severely blocked. When the similarity is large, it means that the river blockage is not serious.

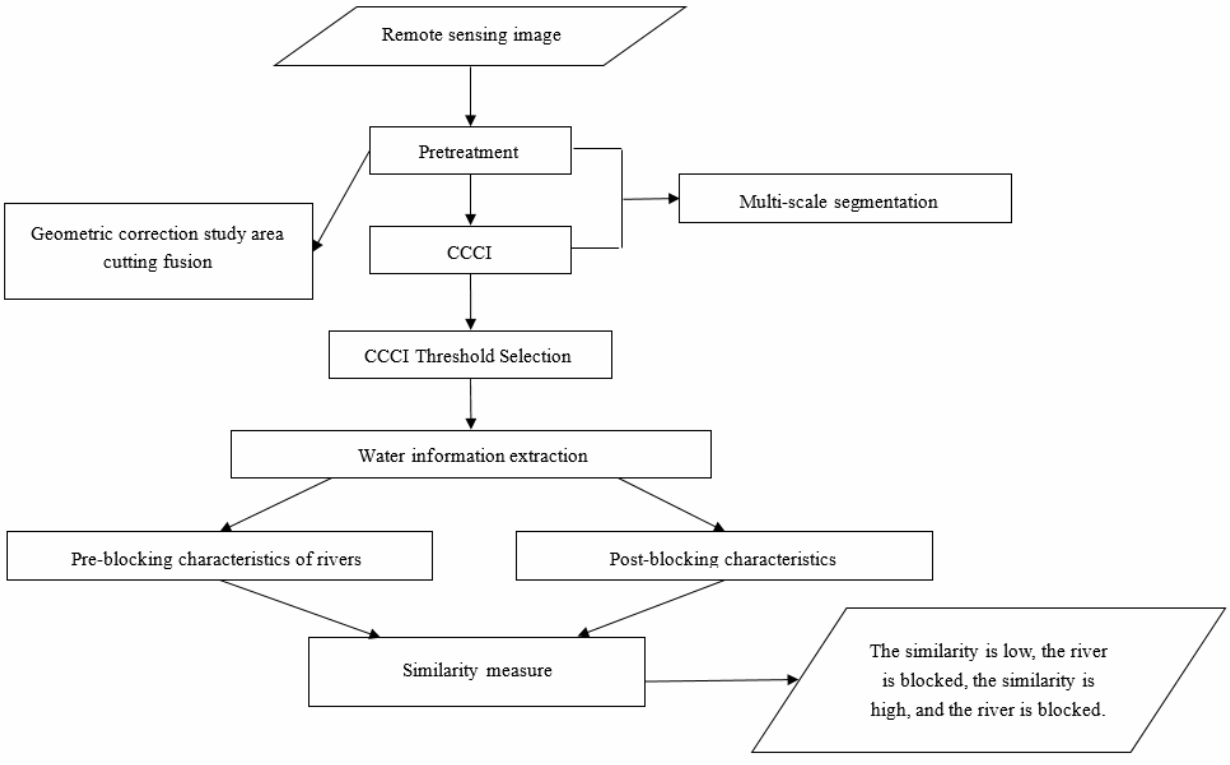

Figure 1. Flow chart of river blocking judgment

4 Experiment

4.1 Datasets

The data set used in this trial was provided by the UK National Defense Science and Technology Laboratory (Figure 2 shows a partial 3-channel satellite imagery of the dataset). The training set contains 25 high-resolution satellite images of 1 square kilometer area. There are three versions of the training set image to choose from, namely grayscale, 3-channel RGB color map and 16-channel image. See Table 1 for details.

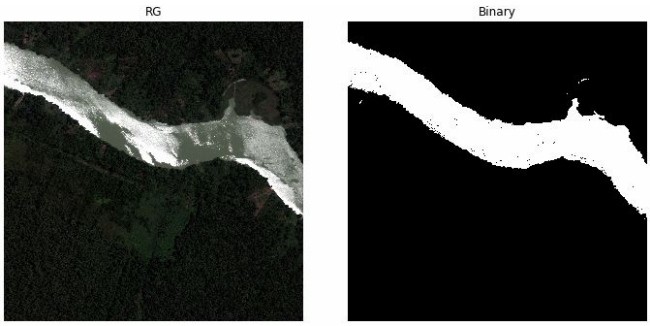

Figure 2. 6050_2_1 river feature extraction

Table 1. Datasets contains content overview

TYPES	BANDS	PIXEL RESOLUTION	CHANNELS	SCALE
GRAYSCALE	PANCHROMATIC BAND	0.31m	1	3348×3392
3 CHANNELS	RGB	0.31m	3	3348×3392
16 CHANNELS	MULTISPECTRAL	1.24m	8	837×848
16 CHANNELS	NEAR INFRARED	7.5m	8	134×136

The flow chart of this experiment is shown in Figure 1 above. The remote sensing image is used for pre-processing, and then CCCI/GMRF/U-net is used to extract the characteristics of the river before and after the blockage, and then the similarity of the image before and after the blockage is judged by using the method of judging image similarity. When the similarity is small, the river is severely blocked. When the similarity is large, it means that the river blockage is not serious.

By adjusting and aligning the 16-channel image to match the 3-channel RGB image, a calibration operation is necessary to eliminate the difference between the channels. Finally, the training focuses on three versions of the image and integrates it into a 20-channel input image.

4.2 Experimental Process

This experiment used 3 band and 16 band images to perform experiments (The 3-band images are the traditional RGB natural color images. The 16-band images contain spectral information by capturing wider wavelength channels. Because the 3-band and 16-band images are colored, the color characteristics of the river can be extracted. This is necessary for CCCI. Images of other bands, such as full-color remote sensing images, have only one color, for example, pure black and white.), using the method mentioned in section 3.1 to calculate the CCCI index, Selecting the appropriate screening threshold in the HSV color histogram (here set to 0.15). And using three latitude and longitude coordinates on the remote sensing image to determine that the two remote sensing images are taken at the same position and are shot at the same height (using 0.5 m Remote sensing image of resolution). The image is divided into 1024×1024 small images for training. The binary image of the river after the earthquake is extracted and the binary map corresponding to the image of the river before the earthquake is used for similarity measurement. The above process is continuously repeated until the thresholds with the highest average similarity of the two binary images and their corresponding CCCI indexes are obtained.

In order to improve the classification accuracy between the water body and the non-water body, the CCCI weight is set to 1.5. According to the actual situation of the experimental area, the segmentation scale is continuously tested, and the segmentation scale is selected to be 256, 512, and 1024 for comparison. When the segmentation scale is 256, although the water body and the mountain body shadow segmentation are separated to a great extent, the large water body and other vegetation bare land are too broken; when the segmentation scale is 512, although the large water body and the tributary are relatively complete, However, there is more mixing of water bodies and mountain shadows. Therefore, this paper considers selecting 1024 as the optimal segmentation scale, with a shape weight of 0.1 and a compactness and smoothness of 0.5.

We used the Swain image database to run a color constant color indexing algorithm in our experiments. The complete database data set of the image is displayed in color. The CCCI algorithm imposes very few restrictions on objects, except that they are multi-colored. The location and orientation of a river can vary in many data sets, its shape can be changed, and even some occlusion can be tolerated, for example when vegetation covers a river. The two-dimensional position and orientation have no effect on the histogram, so they have no effect on the match. Changing the shape of the color area also keeps the

histogram unchanged; however, occlusion affects the histogram and may reduce the confidence of the match. Of course, for the CCCI algorithm, the lighting conditions of the object and the model must be the same. Again, the dimensions must remain approximately the same, which means that the distance between the camera and the object must be similar to the distance of the model.

We eliminated 11 of the 66 model images of the CCCI with saturated response because the ratio with respect to saturated pixels could not be expected to be constant. Then, for our test, a histogram containing 55 images and a second set of 24 different images of the same object took different positions and directions to match the database. Two test objects are shown in Figure 2 and Figure 3.

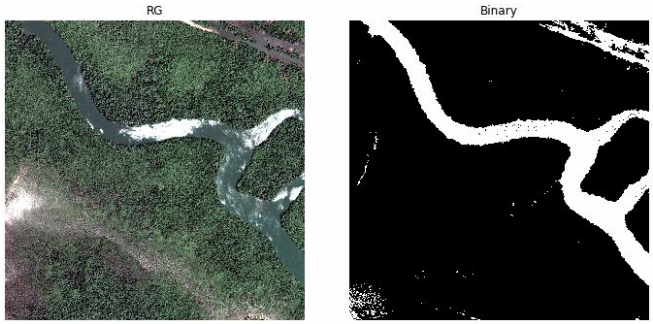

Figure 3. 6080_1_1 river feature extraction

4.3 Experimental Results and Analysis

In the end, we took two 3-channel satellite imagery tests (as shown in Figure 2 and Figure 3). Each satellite image shows the geomorphology of different areas of 1 square kilometer. The upper part of the test results shows the real label. In the river area labeled, the two graphs in the lower half show the model predictions. From the comparison of the real results and the predicted results in the three images, we can conclude that our model can't completely mark all the rivers in the satellite image during the process of predicting the river in the satellite image, but the model is almost Compared with real artificially labeled rivers, rivers in other satellite images can be well predicted during actual use.

CCCI training accuracy and test accuracy are shown in Figure 4(a). The figure shows that the training accuracy and test accuracy are the fastest growing in the first 30 training Epochs. Training tends to converge after the 70th Epochs. In the 100th Epochs, the training accuracy was 85% and the test accuracy was 80%. The color constant color index performs very well. Most river images are correctly identified and have high tolerances.

The effect of threshold selection on model accuracy is shown in Figure 4(b). The figure shows the process of finding the best CCCI Index during training. It can be seen that the optimal feature extraction parameters are selected when the threshold is 0.15.

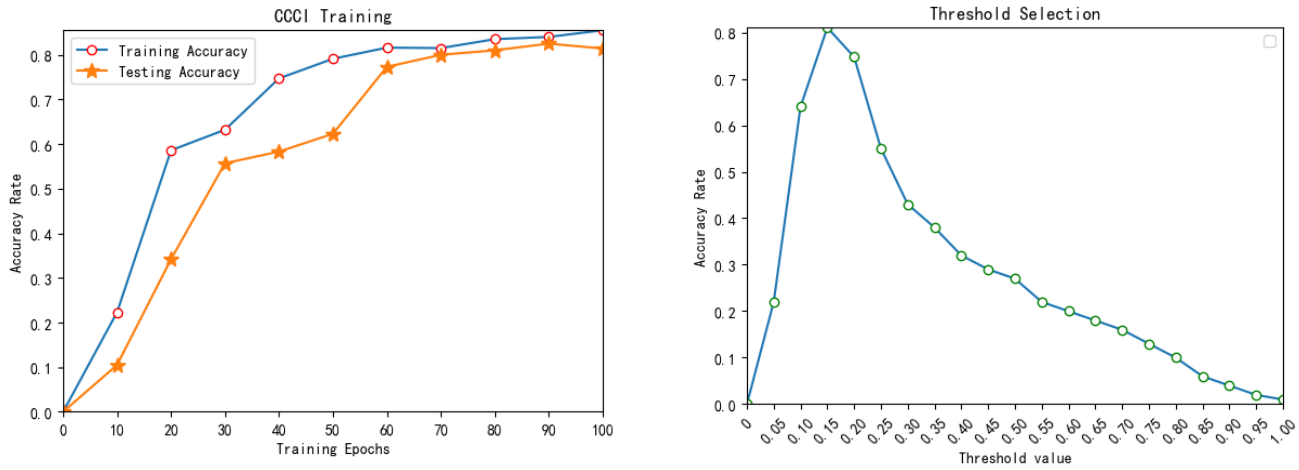

(a) CCCI training accuracy and test accuracy

(b) the impact of threshold selection on model accuracy

Figure 4.

The effect of RGB, Multispectral, and Near Infrared Spectra selection on training accuracy in the dataset is shown in Figure 5(a). It can be seen from the figure that the simultaneous participation of images in the RGB, Multispectral and Near Infrared Spectra bands helps to improve the final accuracy of the model.

The comparison of the training methods of CCCI, GMRF and U-net is shown in Figure 5(b). The water body information is extracted by the CCCI water body extraction method, the GMRF water body extraction method and the U-net water body extraction method respectively. In this paper, the results of manual interpretation are taken as the standard, and the accuracy of the extraction results is evaluated from visual interpretation to quantitative statistics. By comparison, it is found that the overall effect of CCCI

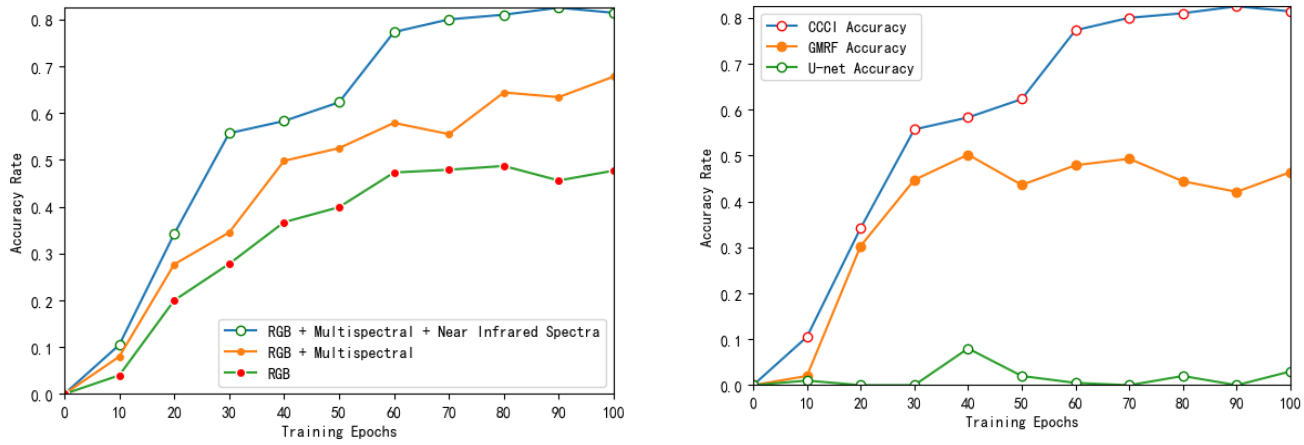

(a) (b)

Figure 5. It shows the effect of the RGB, Multispectral, and Near Infrared Spectra selections on training accuracy in the dataset. The picture on the right is a comparison of the training methods of CCCI, GMRF and U-net

water extraction method is better than the other two extraction methods. CCCI method has better effect on contour extraction, and is hardly affected by vegetation and mountain. It can be seen from the figure that U-net super-neural segmentation has almost nothing to do in extracting river features. The GMRF-based water body extraction method, when the water body is greatly affected by the shadow of the mountain, there is a phenomenon of water body over-lifting and "Noise water body"; in the south of the water body, it is affected by thin clouds, and there is water leakage phenomenon; and object-oriented CCCI water body extraction The method is based on eliminating the effects of thin clouds and hillshading. The accuracy of the extraction is quantitatively judged by the rate of mis-extraction, including the over-extraction rate and the miss-out rate. The over-extraction rate is the ratio of the number of pixels that are actually incorrectly extracted as water bodies to the total number of true water-like pixels in the water body; It is the ratio of the number of pixels that are actually divided into water bodies to the total number of real pixels in the water body. Since the size of the water body is not fixed, it varies with the seasons and other factors. Therefore, the number of water body pixels manually interpreted is the total number of real water pixels. The water extraction method based on GMRF is affected by the shadow of the mountain and the thin cloud, and the leakage rate and over-extraction rate are higher than the CCCI water body extraction method. Therefore, compared with texture feature extraction, color feature extraction CCCI is more suitable for the extraction of river features. To demonstrate the advancement of the method we use for river feature extraction, as shown in Figure 6, we validated river feature extraction on LY datasets[3] by CCCI. It can be seen that CCCI has a good fine-grained performance on the river segmentation results on the LY datasets.

Since the image similarity measure has strong subjectivity, it is not easy to objectively evaluate the performance of an image similarity measure algorithm. When performing image similarity metrics, there are one or more characterization methods and similar metrics, which require a comprehensive evaluation of the similarity measures of different image features or feature combinations and different similarity measures. Compare the performance of different methods and find the best way. Listed below are the criteria for judging several accepted image similarity metric algorithms.

Precision and recall are the most widely cited evaluation criteria in CCCI. The precision is the ratio of the number of related images returned by the system to the number of all returned images in a query process. If there are many correct correlation images in the similarity measurement result set, the precision is high. The recall rate refers to the ratio of the number of related images in the query result returned by the system to the number of all relevant images in the image library (including returned and not returned). The precision and recall rates are shown in Table 2 below.

[3] The LY datasets was produced by the Computer Vision and Artificial Intelligence Laboratory of University of Shanghai for Science and Technology. Its original satellite data is derived from China Gaojing-1 satellite. The original image has a full-color resolution of 0.5 m and a multi-spectral resolution of 2 m. The data set is subject to third party privacy and copyright, except for the parts shown in this article, the rest will not be allowed to be published on the Internet.

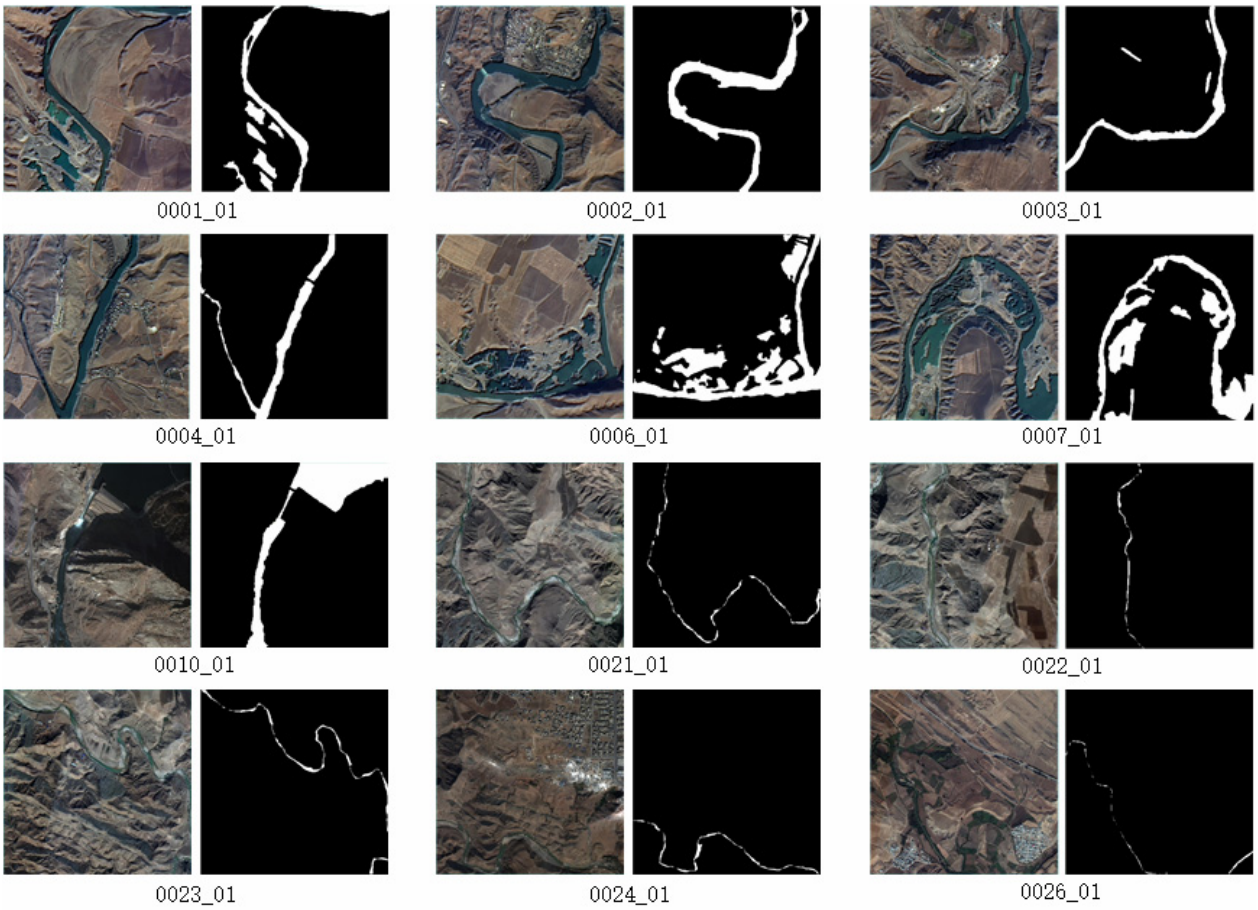

Figure 6. The CCCI method shows 12 groups of river segmentation results on the third-party dataset: the left side of each group of subgraphs is the original satellite imagery, and the right side is the binary map of the river segmentation results extracted by CCCI

Table 2. Select two non-overlapping sub-images of 256×256 size from the 512×512 size image to analyze the precision and recall rate

Image ID	Similarity Measurement Based on Color		Similarity Measurement Based on Texture	
	Precision	Recall	Precision	Recall
6015_3_4	**83.2%**	79.5%	64.9%	60.2%
6080_1_1	**77.9%**	74.6%	54.8%	49.3%

The percentage of blocking degree is a practical discriminating method. Two non-overlapping sub-images of 256×256 size are selected from the image of 512×512 size, and one pair is taken as the query image and the other is taken as the target image. In the case of an ideal similarity measure, the target image should rank first in the similarity measure. The percentage of blockage is shown in Table 3 below.

Table 3. Measurement of the degree of river blockage of 6015_3_4 and 6080_1_1 by various similarity measures

Image ID	Similarity Measurement Based on Color					Similarity Measurement Based on Texture		
	Minkowsky distance	Histogram intersection method	Quadratic distance	χ^2 statistics	Center distance	Mahalanobis distance	Non-geometric similarity measure	Normalized similarity measure
6015_3_4	**21.5%**	20.1%	21.2%	22.8%	21.8%	34.5%	33.3%	33.8
6080_1_1	**8.3%**	9.8%	8.1%	8.0%	11.1%	25.7%	26.2%	25.9

The following two binary maps (shown in Figure 7 and Figure 8) are the binary map of the river before the earthquake on the left and the binary map of the river after the earthquake on the right. Simulated dammed lake 1, normal 78.5%, blocking 22.5%. Simulated dammed lake 2, normal 91.7%, blocking 8.3%.

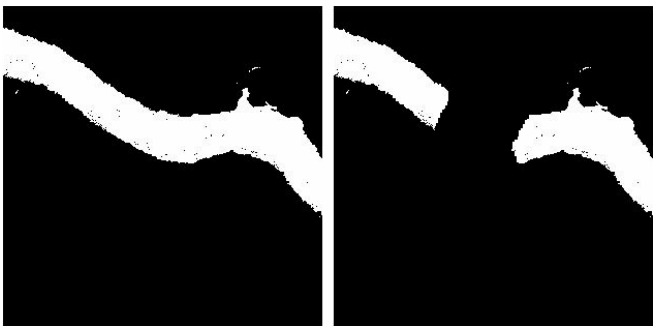

Figure 7. Simulated dammed lake 1, normal 78.5%, blocking 22.5%

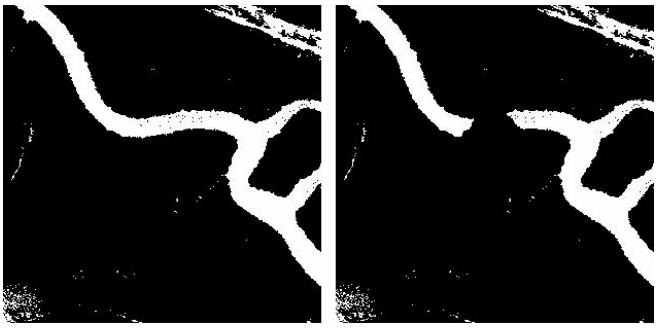

Figure 8. Simulated dammed lake 2, normal 91.7%, blocking 8.3%

5 Conclusion

The color constant color indexing algorithm performs well on water feature extraction on various remote sensing images. Although the spectral power distribution of the illuminator has undergone substantial changes, the object is still correctly identified. Through the experiment, CCCI can be applied to the image feature extraction of rivers in a small sample of remote sensing datasets. Then, using three-point positioning and river binary image judgment before and after the earthquake, it can be judged whether the river is Blockage and river blockage. At the same time, other methods were compared in this experiment, but they were not as good as CCCI in the process of actually extracting river characteristics. We attribute it to the following reasons. Texture extraction is susceptible to interference from various textures in complex environments. The data set used in this experiment describes that the part of the river is too small to be segmented using neural networks. In this case, only the color of the river can be used as the only distinctive feature distinguishing itself from the environment, so it is very effective to compare the color based on the color of the adjacent position.

6 Future Work and Prospects

Further, the vegetation index (SAVI) can be used to judge the local landslide after the earthquake. According to the spectral characteristics of the vegetation, the visible and near-infrared bands of the satellite are combined to form various vegetation indices. Vegetation index is a simple, effective and empirical measure of surface vegetation status. More than 40 vegetation indices have been defined and widely used in global and regional land cover, vegetation classification and environmental change, primary productivity analysis, crops and Pasture estimation, drought monitoring, etc.; and has been integrated into interactive biosphere models and production efficiency models as part of a global climate model; and is widely used for terrestrial applications such as early warning systems for famine; vegetation indices can also Convert to a canopy biophysical parameters. Landslides are often accompanied by the bareness of local geotechnical areas and form a sharp contrast with the surrounding vegetation. By using SAVI to compare the binary images of the post-earthquake vegetation, it is possible to determine whether a landslide has occurred.

Acknowledgements

The authors would like to appreciate all anonymous reviewers for their insightful comments and constructive suggestions to polish this paper in high quality. Thanks to Beijing Hang Tian Shi Jing company, Aerospace Information Research Institute, Chinese Academy of Sciences, and the original satellite remote sensing data provided by the Operation and Maintenance Office of the National Integrated Earth Observation Data Sharing Platform of the Ministry of China Science and Technology. This research was supported by the National Key Research and Development Program of China (No. 2018YFC0810204), National Natural Science Foundation of China (No. 61872242, 61502220), Shanghai Science and Technology Innovation Action Plan Project (17511107203, 16111107502) and Shanghai key lab of modern optical system.

References

[1] P. Vikhar, P. Karde, Improved CBIR System Using Edge Histogram Descriptor (EHD) and Support Vector Machine (SVM), *International Conference on Ict in Business Industry & Government*, Indore, India, 2016, pp. 1-5.

[2] X. Xue, C. Wu, Z. Sun, Y. Wu, N. N. Xiong, Vegetation Greening for Winter Oblique Photography Using Cycle-Consistence Adversarial Networks, *Symmetry*, Vol. 10, No. 7, 294, July, 2018.

[3] C. Reta, J. A. Cantoral-Ceballos, I. Solis-Moreno, J. A. Gonzalez, R. Alvarez-Vargas, N. Delgadillo-Checa, Color Uniformity Descriptor: An Efficient Contextual Color Representation for Image Indexing and Retrieval, *Journal of*

Visual Communication & Image Representation, Vol. 54, pp. 39-50, July, 2018.

[4] M. J. Swain, D. H. Ballard, Color Indexing, *International Journal of Computer Vision*, Vol. 7, No. 1, pp. 11-32, November, 1991.

[5] M. L. Manna, F. Kine, E. Breitbach, J. Jackson, T. Sultan, A. Velten, Error Backprojection Algorithms for Non-Line-of-Sight Imaging, *IEEE Transactions on Pattern Analysis & Machine Intelligence*, Vol. 41, No. 7, pp. 1615-1626, July, 2019.

[6] H. Zhang, J. Tang, R. Wang, Y. Deng, W. Wang, N. Li, An Accelerated Backprojection Algorithm for Monostatic and Bistatic SAR Processing, *Remote Sensing*, Vol. 10, No. 1, 140, January, 2018.

[7] W. S. Chen, M. L. Huang, C. M. Wang, Optimizing Color Transfer Using Color Similarity Measurement, *IEEE/ACIS International Conference on Computer & Information Science*, Okayama, Japan, 2016, pp. 1-6.

[8] M. J. Swain, D. H. Ballard, Indexing via Color Histograms, *International Conference on Computer Vision*, Osaka, Japan, 1990, pp. 390-393.

[9] J. Zhang, J. Geng, J. Wan, Y. Zhang, M. Li, J. Wang, N. N. Xiong, An Automatically Learning and Discovering Human Fishing Behaviors Scheme for CPSCN, *IEEE Access*, Vol. 6, pp. 19844-19858, March, 2018.

[10] B. V. Funt, G. D. Finlayson, Color Constant Color Indexing, *IEEE Transactions on Pattern Analysis & Machine Intelligence*, Vol. 17, No. 5, pp. 522-529, May, 1995.

[11] M. B. Cardenas, M. Doering, D. S. Rivas, C. Galdeano, B. T. Neilson, C. T. Robinson, Analysis of the Temperature Dynamics of a Proglacial River Using Time-lapse Thermal Imaging and Energy Balance Modeling, *Journal of Hydrology*, Vol. 519, pp. 1963-1973, November, 2014.

[12] L. Shen, H. Tang, S. Wang, L. Zhang, River Extraction from the High Resolution Remote Sensing Image Based on Spatially Correlated Pixels Template and Adboost Algorithm, *Acta Geodaetica et Cartographica Sinica*, Vol. 42, No. 3, pp. 344-350, June, 2013.

[13] L. Xu, X. Hou, River Extracted from Remote Sensing Images Based on Region Growing, *Geomatics & Spatial Information Technology*, Vol. 38, No. 3, pp. 198-200, March, 2015.

[14] M. N. Carney, W. M. Johnston, A Novel Regression Model From RGB Image Data To Spectroradiometric Correlates Optimized For Tooth Colored Shades, *Journal of Dentistry*, Vol. 51, pp. 45-48, August, 2016.

[15] K. Zhang, A. Zhang, C. Li, Nutrient Deficiency Diagnosis Method for Rape Leaves Using Color Histogram on HSV Space, *Transactions of the Chinese Society of Agricultural Engineering*, Vol. 32, No. 19, pp. 179-187, October, 2016.

[16] N. Schlömer, *Algorithmic Improvements for the CIECAM02 and CAM16 Color Appearance Models*, https://arxiv.org/abs/1802.06067.

[17] Y. N. Vodyanitskii, N. P. Kirillova, Application of the CIE-L*a*b* System to Characterize Soil Color, *Eurasian Soil Science*, Vol. 49, No. 11, pp. 1259-1268, November, 2016.

[18] K. Kumar, J. P. Li, Zain-Ul-Abidin, Complementary Feature Extraction Approach in CBIR, *International Computer Conference on Wavelet Active Media Technology & Information Processing*, Chengdu, China, 2015, pp. 192-197.

[19] M. Bilal, Algorithmic Optimization of Histogram Intersection Kernel SVM-based Pedestrian Detection Using Low Complexity Features, *IET Computer Vision*, Vol. 11, No. 5, pp. 350-357, August, 2017.

[20] H. Xu, M. Liao, Cluster-based Texture Matching for Image Retrieval, *International Conference on Image Processing*, Chicago, IL, USA, 1998, pp. 766-769.

[21] X. Jiang, Z. Fang, N. N. Xiong, Y. Gao, B. Huang, J. Zhang, L. Yu, P. Harrington, Data Fusion-based Multi-object Tracking for Unconstrained Visual Sensor Networks, *IEEE Access*, Vol. 6, pp. 13716-13728, January, 2018.

[22] R. Khwildi, M. Hachani, A. O. Zaid, A New Indexing Method of HDR Images Using Color Histograms, *Society of Photo-optical Instrumentation Engineers*, Vol. 10341, 1034122, March, 2017.

[23] X. Xu, T. Tan, F. Xu, An Improved U-Net Architecture for Simultaneous Arteriole and Venule Segmentation in Fundus Image, in: M. Nixon, S. Mahmoodi, R. Zwiggelaar (Eds.), *Medical Image Understanding and Analysis*, Springer International Publishing, 2018, pp. 333-340.

[24] V. Iglovikov, A. Shvets, *TernausNet: U-Net with VGG11 Encoder Pre-Trained on ImageNet for Image Segmentation*, https://arxiv.org/abs/1801.05746.

[25] E. J. Hong, A. Saudi, J. Sulaiman, Numerical Assessment for Poisson image Blending Problem Using MSOR Iteration via Five-point Laplacian Operator, *Journal of Physics: Conference Series*, Vol. 890, No. 1, 012010, 2017.

[26] S. K. Ghosal, J. K. Mandal, R. Sarkar, High Payload Image Steganography Based on Laplacian of Gaussian (LoG) edge detector, *Multimedia Tools & Applications*, Vol. 77, No. 23, pp. 30403-30418, December, 2018.

[27] N. L. C. Junior, A Fuzzy c-means Algorithm Based on an Adaptive L2 Minkowsky Distance, *International Conference on Hybrid Intelligent Systems*, Rio de Janeiro, Brazil, 2005, pp. 104-109.

[28] F. Baji, M. Mocanu, Connected Components Objects Feature for CBIR, *International Carpathian Control Conference*, Sinaia, Romania, 2017, pp. 545-550.

[29] J. Hafner, H. S. Sawhney, W. Equitz, M. Flickner, W. Niblack, Efficient Color Histogram Indexing for Quadratic Form Distance Functions, *IEEE Transactions on Pattern Analysis & Machine Intelligence*, Vol. 17, No. 7, pp. 729-736, July, 1995.

[30] W. X. Bao, G.-F. Yu, G.-S. Hu, M. Zhu, Image Matching Algorithm Based on Mahalanobis-Distance Spectral Features, *Journal of South China University of Technology*, Vol. 45, No. 10, pp. 114-120 &128, October, 2017.

Biographies

Chunxue Wu is a Professor with the Computer Science and Engineering and software engineering Division, School of Optical-Electrical and Computer Engineering, University of Shanghai for Science and Technology, China. His research interests include, wireless sensor networks, distributed and embedded systems, wireless and mobile systems, networked control systems.

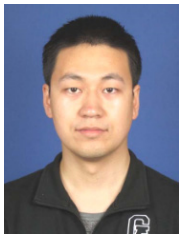

Bobo Ju is a master's student in computer science and technology at University of Shanghai for Science and Technology. He is engaged in big data and artificial intelligence research under the guidance of Professor Chunxue Wu. Addr. Jungong road. 516, Shanghai, China, 200093.

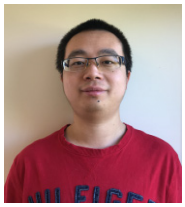

Yan Wu is currently a postdoctoral associate at the school of public and environmental affairs, Indiana University Bloomington. His research involves elucidations of environmental fate of contaminants using chemical and computational techniques, as well as predictions of their associated effects on wildlife and public health. Data Processing and Analysis in Environmental Related Fields.

Xiao Lin received the Ph.D. degree in computer science from the Shanghai Jiao Tong University, Shanghai, China. She is currently an associate professor at the Department of Computer Science, Shanghai Normal University, Shanghai, China. Previously, she engaged in postdoctoral research at the University of Shanghai for Science and Technology, Shanghai, China. Her research interests include image processing, computer vision, etc.

Naixue Xiong is currently an Associate Professor (3rd year) at Department of Mathematics and Computer Science, Northeastern State University, OK, USA. Before he attended Northeastern State University, he worked at Georgia State University, wentworth Technology Institution, and Colorado Technical University about 10 years. His research interests include Cloud Computing, Security and Dependability, Parallel and Distributed Computing, Networks, and Optimization Theory.